Ocean Sci., 18, 129–142, 2022
https://doi.org/10.5194/os-18-129-2022

Ocean Science Open Access EGU

Characterization of the Atlantic Water and Levantine Intermediate Water in the Mediterranean Sea using 20 years of Argo data

Giusy Fedele, Elena Mauri, Giulio Notarstefano, and Pierre Marie Poulain

National Institute of Oceanography and Applied Geophysics, OGS, 34010 Sgonico (TS), Italy

Correspondence: Giusy Fedele (gfedele@inogs.it)

Received: 4 July 2021 – Discussion started: 9 July 2021
Revised: 27 November 2021 – Accepted: 30 November 2021 – Published: 26 January 2022

Abstract. Atlantic Water (AW) and Levantine Intermediate Water (LIW) are important water masses that play a crucial role in the internal variability of the Mediterranean thermohaline circulation. To be more specific, their variability and interaction, along with other water masses that characterize the Mediterranean basin, such as the Western Mediterranean Deep Water (WMDW), contribute to modify the Mediterranean Outflow through the Strait of Gibraltar, and hence they may influence the stability of the global thermohaline circulation.

This work aims to characterize AW and LIW in the Mediterranean Sea, taking advantage of the large observational dataset (freely available on https://argo.ucsd.edu, https://www.ocean-ops.org, last access: 17 January 2022; Wong et al., 2020) provided by Argo floats from 2001 to 2019. AW and LIW were identified using different diagnostic methods, highlighting the inter-basin variability and the strong zonal gradient that both denote the two water masses in this marginal sea. Their temporal variability was also investigated over the last 2 decades, providing a more robust view of AW and LIW characteristics, which have only been investigated using very short periods in previous studies due to a lack of data.

A clear salinification and warming trend characterize AW and LIW over the last 2 decades ($\sim 0.007 \pm 0.140$ and $0.006 \pm 0.038\,\mathrm{yr}^{-1}$; 0.026 ± 0.715 and $0.022 \pm 0.232\,^{\circ}\mathrm{C\,yr}^{-1}$, respectively). The salinity and temperature trends found at sub-basin scale are in good agreement with previous results. The strongest trends are found in the Adriatic basin in the properties of both AW and LIW.

1 Introduction

Atlantic Water (AW) and Levantine Intermediate Water (LIW) play a central role in the internal variability of the Mediterranean thermohaline circulation, contributing to the dense water formation in this enclosed basin (Tsimplis et al., 2006). The variability and interaction of these two water masses modulate the Mediterranean outflow through the Gibraltar Strait, which plays an important role in North Atlantic oceanic variability and in turn in the stability of the global thermohaline circulation (e.g. Rahmstorf, 2006; Hernández-Molina et al., 2014). Therefore, from a climatic point of view, it is relevant to characterize their main properties and monitor their variability, which is the main purpose of this paper.

Flowing into the Mediterranean Sea through the Gibraltar strait, AW is less dense than the surrounding water masses, and it therefore populates most of the Mediterranean surface layer. Its path is mainly driven by the Coriolis effect and by the complex topography that characterizes this region (Millot and Taupier-Letage, 2005).

LIW is the most voluminous water mass produced in the Mediterranean Sea (e.g. Skliris, 2014; Lascaratos et al., 1993), and it is the saltiest water formed with a relatively high temperature at intermediate depths. It is formed in the Levantine sub-basin after which it is named, where one of the main formation sites is the Rhodes Gyre (e.g. Tsimplis et al., 2006; Kubin et al., 2019). LIW strongly influences the thermohaline circulation, flowing at intermediate depths and then passing over the sills, exiting the Gibraltar Strait, and modifying the Atlantic circulation (Rahmstorf, 1998; Bethoux et al., 1999).

Several studies have been devoted to the analysis of the main features and variability of AW and LIW, taking advan-

tage of different indicators to identify and track these two water masses in the Mediterranean Sea. Among these, AW and LIW are usually referred to the minimum and maximum salinity in the surface and intermediate layers of the water column, respectively (e.g. Millot and Taupier-Letage, 2005; Bergamasco and Malanotte-Rizzoli, 2010; Mauri et al., 2019; Juza et al., 2019; Kokkini et al., 2019; Vargas-Yáñez et al., 2020). However, different approaches can also be found in the literature. To be more specific, Millot (2014) associated LIW with the maximum of the potential temperature vertical gradient found in an intermediate water layer, while Bosse et al. (2015) identified LIW in the northwestern Mediterranean Sea with the maximum salinity value found between two potential density values ($\sigma_\theta = [29.03–29.10]\,\mathrm{kg\,m^{-3}}$), encompassing both temperature and salinity maxima characterizing the LIW layer. The main findings related to the hydrological properties of these two water masses are summarized below.

AW enters into the Mediterranean Sea through the Gibraltar Strait, occupying the upper 200 m of depth with potential density, temperature, and salinity annual mean values: $\sigma_\theta \cong [26.5–27]\,\mathrm{kg\,m^{-3}}$, $T \cong [14–16]\,^\circ\mathrm{C}$, and $S \cong [36.0–36.5]$, respectively (e.g. Bergamasco and Malanotte-Rizzoli, 2010; Hayes et al., 2019). AW flowing at the surface continuously interacts with the atmosphere and is subject to evaporation and mixing with the underlying water masses. Flowing eastward, it becomes denser and the minimum salinity core sinks. Therefore, it can be capped by the surface mixed layer and less influenced by air–sea interactions. Its properties and variability are also modified by the local eddies and by the river discharges in the coastal regions. These mechanisms shape the AW, leading to an increase of salinity from about 36.25 in the Strait of Gibraltar to values around 39.2 in the Levantine Sea (e.g. Bergamasco and Malanotte-Rizzoli, 2010; Hayes et al., 2019). These values highlight strong AW temperature and salinity gradients between the western Mediterranean (WMED) and the eastern Mediterranean (EMED).

The properties of the LIW core in the WMED are commonly referred to the following ranges of potential density, temperature, salinity and depth, respectively: $\sigma_\theta = [29–29.10]\,\mathrm{kg\,m^{-3}}$, $T = [13–14.2]\,^\circ\mathrm{C}$, $S = [38.4–38.8]$, and $D = [200–600]\,\mathrm{m}$ (e.g. Millot, 2013; Hayes et al., 2019; Vargas-Yáñez et al., 2020). In contrast, in the EMED these properties span over different values: $\sigma_\theta = [28.85–29.15]\,\mathrm{kg\,m^{-3}}$, $T = [14.6–16.4]\,^\circ\mathrm{C}$, $S = [38.85–39.15]$, and $D = [150–400]\,\mathrm{m}$ (e.g. Lascaratos et al., 1993; Hayes et al., 2019). Therefore, moving westward T and S decrease and LIW sinks.

These studies provide a general view of AW and LIW properties in the Mediterranean Sea, highlighting a strong inter-basin variability of these water masses along their paths, which in turn influences their temporal changes.

An example is given by a recent paper by Kassis and Korres (2020), which provides a detailed view of the EMED hydrographic properties for the period 2004–2017 taking advantage of Argo data. Exploring the water column from the surface down to 1500 m in seven different regions of the EMED, they revealed a high inter-annual variability of the stored heat and salt over this region.

In this study, by following a similar approach we investigate AW and LIW properties, isolating their main characteristics and variability from the surrounding water masses, taking advantage of several diagnostics discussed in Sect. 2.2. Our work aims to provide a more robust view of AW and LIW characteristics, which in previous studies have only been investigated over short periods due to lack of data.

In the frame of climate change studies, it is important to estimate possible impacts of AW and LIW changes on the Mediterranean climate, since this region is one of the most vulnerable climate change hotspots (Giorgi, 2006). In fact, changes in temperature and salinity can strongly affect the marine system over the Mediterranean and related human activities.

Previous studies highlighted a clear salinification of the Mediterranean Sea over the past few decades (e.g. Painter and Tsimplis, 2003; Vargas-Yáñez et al., 2010; Schroeder et al., 2017; Skliris et al., 2018) and a clear deep water warming trend after the 1980s, which in the literature is often related to the Nile River damming and global warming (Vargas-Yáñez et al., 2010). Positive temperature and salinity trends, oscillating between $[0.0016/0.0091]\,^\circ\mathrm{C\,yr^{-1}}$ and $[0.0008/0.001]\,\mathrm{yr^{-1}}$, respectively, are found in the deep layer (below ~ 700 m) between 1950 to 2005 (e.g. Bethoux et al., 1990; Rohling and Bryden, 1992; Millot et al., 2006; Vargas-Yáñez et al., 2010; Borghini et al., 2014).

This observed salinification and warming are also found at intermediate depths in several studies (e.g. Zu et al., 2014; Schroeder et al., 2017; Skliris et al., 2018), with ranges that depend on the region of investigation. A clear positive salinity trend between 150–600 m is found in the Mediterranean Sea by Skliris et al. (2018), analysing the MEDATLAS data from 1950 to 2002 ($\sim 0.007 \pm 0.004\,\mathrm{yr^{-1}}$).

In contrast, heterogeneous temperature trends are found in the upper layer in different regions (Painter and Tsimplis, 2003). This sensitivity of the trends to the area of interest can be due to several reasons, such as the changes in the large-scale atmospheric forcing of the Mediterranean region, the river runoff (which differs from one region to another), and the data coverage over a specific area (e.g. Painter and Tsimplis, 2003; Vargas-Yáñez et al., 2009, 2010). In this respect, Vargas-Yáñez et al. (2009) highlighted that the scarcity of data makes trend estimations very sensitive to the data post-processing, comparing results from different studies dealing with the same time period. Therefore, in order to reduce the uncertainty of the trend estimations, longer and less sparse time series are needed.

In this respect, this work aims to provide an updated view of the temporal evolution and trends of the AW and LIW, taking advantage of the large observational dataset provided by the MedArgo Program (Poulain et al., 2007). It covers the

water column from the surface down to ∼2000 m over the entire Mediterranean basin from 2001 to 2019. The Mediterranean Sea has been widely studied through the deployment of hundreds of Argo profiling floats (Argo, 2020) over the last 2 decades as part of various national, European, and global programmes (Wong et al., 2021) and with the participation of different institutions. For these reasons, this dataset constitutes an optimal observational framework to investigate AW and LIW properties.

The dataset and the methods used in this study are described in Sect. 2, and the results are presented in Sect. 3, where the inter-basin and inter-annual variabilities of AW and LIW in the Mediterranean Sea are shown. The main conclusions are drawn in Sect. 4.

2 Data and method

2.1 Data

In this work the AW and LIW properties in the Mediterranean Sea are investigated taking advantage of the Argo float dataset, which consists of more than 30 000 T–S profiles for the period 2001–2019. Since 2001, the number of observations is generally increasing, reaching a peak of 4188 profiles in 2015, mainly thanks to the combined efforts of national and international Argo initiatives. The deployments of most Argo floats in the Mediterranean were coordinated by the MedArgo regional centre (Poulain et al., 2007). In the Mediterranean, the cycling period is usually reduced to 5 d, and the maximum profiling depth is mostly 700 or 2000 m (Poulain et al., 2007). The floats are equipped with Sea-Bird conductivity–temperature–depth (CTD) sensors (model SBE41CP; https://www.seabird.com/sbe-41-argo-ctd/product-details?id=54627907875, last access: December 2021) with accuracies of ±0.002 °C, ±0.002, and ±2 dbar for temperature, salinity, and pressure, respectively. The data measured by the profilers are transmitted to satellites (e.g. via the Iridium or Argos telemetry systems) and then to ground receiving stations, processed and real-time quality-controlled by the Argo Data Assembly Centres (https://www.euro-argo.eu/Activities/Data-Management/Euro-Argo-Data-Centres, last access: December 2021), and sent to the Global Data Assembly Centre where they are made available for free to users (https://fleetmonitoring.euro-argo.eu/dashboard?Status=Active, last access: December 2021). The delayed-mode quality control applied on pressure, temperature, and salinity follows the guidelines described in the Argo Quality Control Manual for CTD (e.g. Wong et al., 2021; Cabanes et al., 2016), in conjunction with other procedures developed at regional level (Notarstefano and Poulain, 2008, 2013), to check the salinity data and any potential drift of the conductivity sensor.

The analyses are performed in eight Mediterranean sub-basins following the climatological areas defined by the EU/MEDARMEDATLAS II project (http://nettuno.ogs.trieste.it/medar/climatologies/medz.html, last access: December 2021), emphasizing the processes that take place in each sub-basin and that modify water mass properties. Figure 1 shows the geographical distribution of the Argo profiles from 2001 to 2019 in the eight sub-basins considered (Algerian, Catalan, Ligurian, Tyrrhenian, Adriatic, Ionian, Cretan, and Levantine). The Alboran, Aegean, and the Sicily Channel sub-basins are not analysed in this work due to the scarcity of observations in these areas.

Most sub-basins are spatially well covered, except for the Adriatic Sea, where the majority of observations are concentrated in the South Adriatic Pit (SAP), and therefore it is important to keep in mind that the results found for this region are only representative of the southern Adriatic Sea. The SAP is an important deep-water convection site in the Mediterranean Sea (e.g. Kokkini et al., 2019; Mauri et al., 2020; Mihanović et al., 2021; Azzaro et al., 2012; Bensi et al., 2013), and therefore it is also considered a crucial area from a climatic perspective. The temporal distribution of the float data is different in the various sub-basins: the longest time series are available in the Ionian, Cretan, and Levantine regions, with data from 2001 to 2019; followed by the Algerian, Ligurian, and Tyrrhenian sub-basins where data are available after 2003; and then by the Adriatic Sea with data available only after 2009. In this context, it is important to mention that the low density in space and time of the Argo profiles induces uncertainties in the results, especially during the first years of the analysed period.

2.2 Methods

As discussed in the introduction, many indicators and characteristics have been adopted in literature to track AW and LIW in the Mediterranean Sea. Most of them consider the minimum and maximum salinity at surface and intermediate layer for AW and LIW, respectively, as the best indicator, and this motivated us to follow a similar approach (e.g. Millot and Taupier-Letage, 2005; Bergamasco and Malanotte-Rizzoli, 2010; Hayes et al., 2019; Lamer et al., 2019).

A preliminary step in this analysis was the post-processing: we first applied a time sub-sampling on each profiler to obtain a more homogeneous dataset (Notarstefano and Poulain, 2009). This is applied to each float as follows: if the cycling period is 1 d or less, the profiles are sub-sampled every 5 d; if the period is 2 or 3 d, they are sub-sampled every 6 d; and if the period is 5 or 10 d, no subsampling is applied. Afterward, each profile was linearly interpolated from the surface (0 m) to the bottom every 10 m to obtain comparable profiles. Following this, a running filter with a 20 m window was applied to the data along the depth axis to smooth any residual spike.

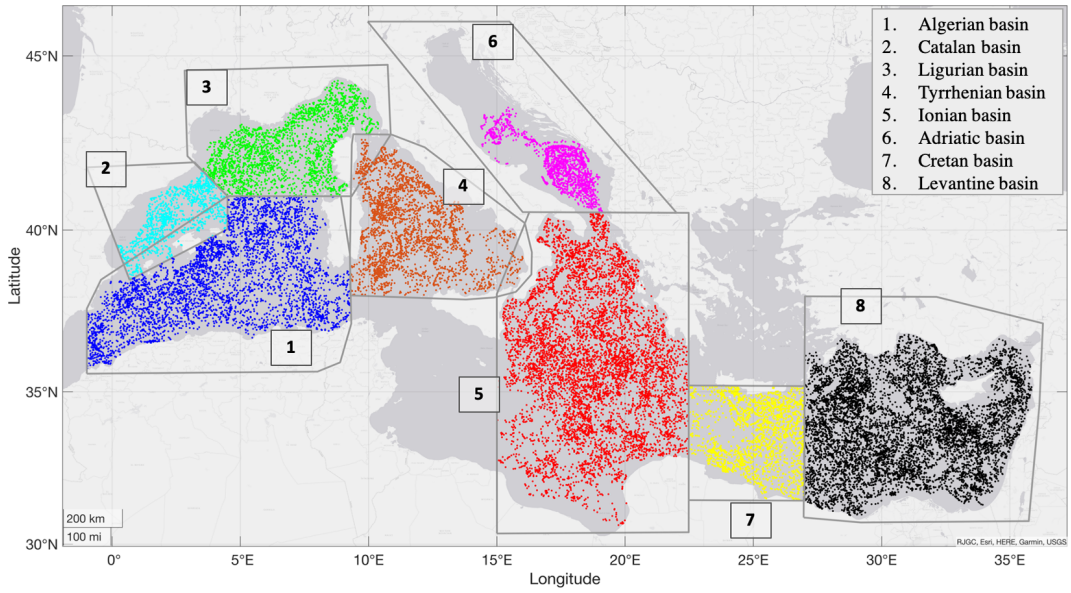

Figure 1. Scatter plot of Argo float profiles in the Mediterranean Sea between 2001 and 2019 in eight regions based on the climatological areas defined by the EU/MEDARMEDATLAS II project. Basemap credits are attributed to RJGC, Esri, HERE, Garmin, USGS.

The minimum and maximum salinity value in each profile is then associated with the AW and LIW core in the respective depth layer. Following this, the correspondent depth and temperature values are considered.

Once the AW and LIW core are identified in each profile, the AW and LIW inter-basin variabilities were analysed by taking advantage of the boxplot approach applied to each parameter and region (Fig. 2). In Fig. 2, the whiskers (dashed black line outside of the box) extend to the most extreme data points not considering the outliers at the 5 % significance level (p value ≤ 0.05). In order to test the significance, Student's t distribution was applied to each hydrological parameter in every sub-basin (Pearson, 1895). The null hypothesis (that states that the population is normally distributed) is rejected with a 5 % level of statistical significance. This method is also applied to the time series trends. In Sect. 3.1 we often refer to the range and skewness of the distributions, which are the difference between the upper and lower limits and the measure of the symmetry of the distributions, respectively (including only the 5 % significance values).

Considering only the AW and LIW salinity, temperature, and depth values at a 95 % level of significance (Fig. 2), as has been done for the spatial analysis, the time series from 2001 to 2019 have been computed in each sub-basin to analyse the low-frequency variability (LFV) and trends at interannual to decadal timescale over the available observed periods. In this respect, the high-frequency variability was filtered out, first by subtracting the mean seasonal cycle to the raw time series and then by applying a median yearly average filter. This last step is needed since the data are not homogeneous in time in every sub-basin from 2001 to 2019, and therefore without it the seasonal variability can contaminate the estimation of the trends. The latter have been computed using the linear least-squares method to fit a linear regression model to the data.

3 Results and discussion

In this section, the AW and LIW properties are investigated in the eight Mediterranean climatic regions mentioned above, focusing on both their spatial and temporal variability. The analysis of the trends and spectral features are also shown.

3.1 Inter-basin variability

3.1.1 AW

The hydrological properties of the AW core in eight sub-basins (Fig. 1) are shown in Fig. 2a, b, and c, providing a compact view of the AW inter-basin variability for each parameter using the boxplot approach.

Moving eastward, the AW salinity increases from ~ 36 to 39.5 (minimum and maximum whiskers limits; Fig. 2a) since the surface salinity minimum is progressively smoothed by horizontal mixing with surrounding saltier waters. In fact, as discussed by Font et al. (1998), the AW minimum salinity is dependent on the different degrees of mixing due to its residence times.

In the Algerian sub-basin, the salinity range reaches the highest extension compared to the other regions, probably due to the large baroclinic instability that produces high mesoscale variability in the surface layer and horizontal mixing by strong eddies (Demirov and Pinardi, 2007).

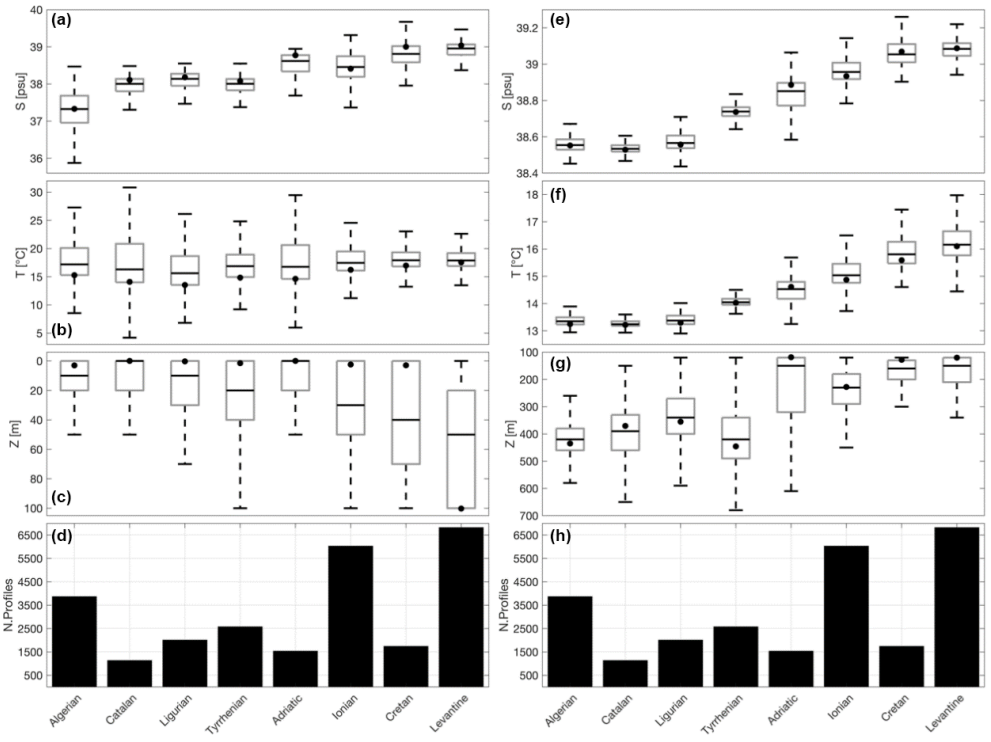

Figure 2. Boxplot diagrams for the AW salinity **(a)**, temperature **(b)**, and depth **(c)** in eight Mediterranean sub-basins. Inside each grey box, the bold black line indicates the median, while the bottom and top edges of the box indicate the 25th and 75th percentiles, respectively, and the black dots show the mode of each distribution, which corresponds to the maximum PDF. The number of profiles (black bars) for each sub-basin is shown in **(d)**. The corresponding diagrams for LIW are shown in **(e)**, **(f)**, **(g)**, and **(h)**.

The AW salinity range is smaller in the Catalan, Ligurian, and Tyrrhenian seas, where similar distributions are found both in terms of range and skewness (which is close to zero): the main mode and the median have salinity of ~ 38. In the Adriatic Sea the distribution is probably skewed toward higher values because a clear positive salinity trend is found (Fig. 3; Lipizer et al., 2014). In the Adriatic, Ionian, and Cretan seas, the range is higher than the surrounding sub-basins: in the Adriatic and Ionian seas this could be associated with the Bimodal Oscillation System (BiOS) and the reversal of the North Ionian Gyre (Rubino et al., 2020), while in the Cretan Sea we speculate that it is caused by the sinking of AW during winter. This is in agreement with Schroeder (2019), where it is shown that the strong wind-induced evaporation and heat loss during winter in the Cretan Sea led the AW transformation into salty and warm Cretan Intermediate Water. The depths reached in the Cretan basin (Fig. 2c) seem to confirm this hypothesis.

The AW temperature is highly variable, ranging between ~ 5 and $\sim 30\,^{\circ}$C, with a wider range in the Catalan and Adriatic regions (Fig. 2b) that is possibly due to the higher seasonal sea surface temperature variability over these sub-basins (Shaltout and Omstedt, 2014). The lowest temperatures detected can be related to the freshwater fluxes in these regions. In this respect, an episode that could be relevant for the AW distribution in the Adriatic Sea is the large river runoff observed in 2014 by Kokkini et al. (2019) that caused a saline stratification for more than a year. This episode is also captured by our analyses (Fig. 3). As observed for the AW salinity mode, even the temperature mode shifts toward higher values moving eastward, in agreement with the literature (Bergamasco and Malanotte-Rizzoli, 2010). In the Algerian basin, the AW temperature mode is higher than it is in the Catalan sub-basin: this could be due to the influence of freshwater fluxes in the Catalan region and led by the high eddy activity over the Algerian region (Escudier et al., 2016), which is in turn led by the strong baroclinic instability already discussed for the salinity field (e.g. Demirov and Pinardi, 2007; Cotroneo et al., 2016; Aulicino et al., 2018, 2019). The temperature and salinity ranges captured in the Algerian region are in good agreement with those found by Cotroneo et al. (2019) and shown in their Table 2.

The depths of the AW core oscillate between 0 and 90 m, with the main mode sinking eastward (Fig. 2c). The distributions are all skewed toward lower depths, with the maximum probability density function (PDF) near the surface and a median shifting from 0 to 45 m moving eastward, indicating a clear sinking of the AW along its pathway.

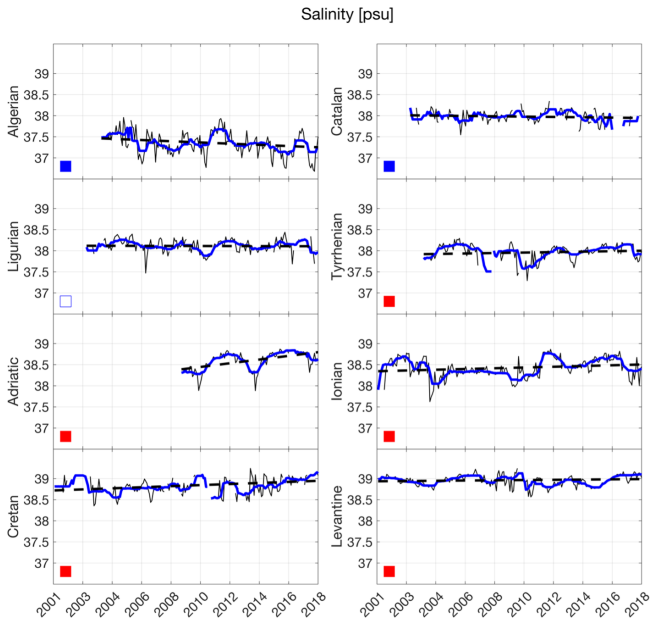

Figure 3. AW salinity time series in eight sub-basins: the thin black lines show the monthly time series (seasonal cycle filtered out), the thick blue lines are the 1-year moving average time series, and the dashed black lines are the trends. The filled red and blue squares identify the positive and negative trends with p value ≤ 0.05, respectively, while the unfilled red and blue squares identify the positive and negative trends with p value > 0.05, respectively.

3.1.2 LIW

In this section, the main hydrological properties of LIW are analysed in each sub-basin.

Flowing away from the region of formation, LIW interacts with the surrounding water masses and becomes less salty; the salinity sharply drops from ~ 39.2 to ~ 38.5, moving from the Levantine to the Ligurian sub-basin, and then it becomes more stable in the Algerian and Catalan regions, oscillating around ~ 38.5 (Fig. 2e). The distributions are highly symmetric around the median, and the variability decreases flowing westward, possibly because LIW becomes deeper, sinking from ~ 100 to ~ 650 m (Fig. 2g). The highest salinity is reached in the Cretan basin, where the formation of salty and warm Cretan Intermediate Water, caused by strong wind-induced evaporation and heat loss during winter, influences the LIW properties and detection (Schroeder, 2019).

The LIW temperature decreases westward from ~ 18 to ~ 12.8 °C. The range is higher in the EMED, as also found for salinity, suggesting that over this region the intrusion of warmer and saltier surface waters due to convective processes characterizes the LIW formation (Fig. 2f; Schroeder, 2019).

The sinking of the LIW flowing westward is shown in Fig. 2g, dropping from about 100 to 650 m (maximum whisker values). The distributions tend to be symmetric in most of the Mediterranean Sea, except for the Adriatic Sea, where a strong LIW bimodality in the depth domain is found, with two peaks located at ~ 190 and ~ 500 m (here not shown), in agreement with Kokkini et al. (2019) and Mihanović et al. (2021). In this respect, Mihanović et al. (2021), analysing observed data from CTD measurements, Argo floats, several glider missions, satellite observations, and operational ocean numerical model products, provide a possible explanation for this double-maxima vertical pattern, suggesting that these two peaks may be explained by two concurrent events: the winter convection at the beginning of 2017, which leads higher salinities in the water column, and a very strong inflow of high-salinity waters from the North Ionian Gyre in late winter and spring of 2017, which this time is almost restricted to the surface.

3.2 Inter-annual variability

In this section, the temporal variability of the AW and LIW in each sub-basin is studied analysing the 1-year moving average time series and the relative trends.

The results of this analysis are affected by the irregular spatial and temporal sampling of the Argo floats. Time gaps in the data are found in the Catalan, Tyrrhenian, and Cretan seas (Fig. 3). The missing data are due to the lack of Argo float samplings. Data in the Adriatic Sea are available only after 2009, while the Ionian, Cretan, and Levantine sub-basins have much longer time series, with data covering the period from 2001 to 2019.

3.3 Trends

3.3.1 AW

The AW salinity temporal evolution is shown in Fig. 3, where significant trends (at 5 % level of significance) are found in each region (Table 1). Positive trends are clearly found in the EMED and in the Tyrrhenian Sea, highlighting a clear salinification of the AW in the last 2 decades over most of the Mediterranean Sea ($\sim 0.007 \pm 0.140\ \mathrm{yr}^{-1}$; Table 1). Comparable positive salinity trends between 0–150 m ($\sim 0.009 \pm 0.009\ \mathrm{yr}^{-1}$) are also found in Skliris et al. (2018), where multi-decadal salinity changes in the Mediterranean Sea are investigated taking advantage of the MEDATLAS database (MEDAR Group, 2002), which consists of temperature and salinity profiles in the Mediterranean from 1945 to 2002 (https://www.bodc.ac.uk/resources/inventories/edmed/report/4651/, last access: December 2021). A clear meridional separation is found in the AW trends during the observed period. In the Tyrrhenian Sea and in the entire EMED the AW becomes saltier, with significant positive trends, whilst in the WMED a significant negative trend emerges in the Algerian and Catalan sub-basins (Table 1). This freshening of the AW inflow could be related to the observed rapid freshening of the North Atlantic Ocean (Dickson et al.,

2002), the causes of which are related to different phenomena, including the accelerating Greenland melting triggered by the global warming (Dukhovskoy et al., 2019). These findings seem in contradiction with the results provided by Millot (2007), which show a salinification of the Mediterranean outflow and were obtained by analysing autonomous CTD measurements on the Moroccan shelf in the Strait of Gibraltar in the period 2003–2007; this contradiction may be caused by the different epochs under study. In fact, comparing Fig. 3 in Millot (2007) and Fig. 3 in this work, a similar positive trend is captured in the Algerian sub-basin in the same period, but when extending the analysis to a longer time series, a clear negative trend leads the AW variability at inter-annual to decadal timescales. Opposite trends are found in the EMED and in the Tyrrhenian sub-basin, where the very strong increase in net evaporation of $\sim 8\,\%$ to $12\,\%$ over 1950–2010 (Skiliris et al., 2018) and the damming of the Nile River (as projected by Nof, 1979) may have caused the AW salinification. The trends are steep in the Adriatic and Cretan sub-basins, where the salinity increases by an order of magnitude ($O[10^{-2}]$), and the largest increase is found in the Adriatic Sea ($0.044 \pm 0.188\,\mathrm{yr}^{-1}$). Here the impact of the negative E–P anomalies and large river runoff observed by Kokkini et al. (2019) around 2014 is well captured by the salinity time series. The results in the EMED are in good agreement with Fig. 9 of Kassis and Korres (2020), where the yearly average salinity per depth zone and per region between 2004–2017 are shown. Similarities in the observed trend in the Ionian Sea ($0.009 \pm 0.181\,\mathrm{yr}^{-1}$) are also found by Zu et al. (2014) (mean trend $\sim 0.011\,\mathrm{yr}^{-1}$), where the Argo float data between 2004 and 2014 are analysed.

According to the above-mentioned meridional salinity transition from negative to positive salinity trends moving eastward, the temperatures also show a meridional shift from positive to negative significant trends east of the Ionian Sea, with a mean positive AW temperature trend over the eight analysed sub-basins ($0.026 \pm 0.715\,^{\circ}\mathrm{C\,yr}^{-1}$; Table 1; Fig. 4). Inter-basin changes between the sub-basins are instead linked to changes in the large-scale meteorological forcing of the Mediterranean region (Painter and Tsimplis, 2003). As found for the salinity field, the sharper increase is related to the Adriatic Sea ($\sim 0.117 \pm 0.951\,^{\circ}\mathrm{C\,yr}^{-1}$), highlighting the presence of mechanisms that enhance the trends over this region. A sharpening in the trend over the last decade is captured in the Catalan sub-basin (Fig. 7) and confirmed by Schuckmann et al. (2019), who observed the same behaviour in the northwestern Mediterranean with a trend over the last decade ($\sim 0.047\,^{\circ}\mathrm{C\,yr}^{-1}$) that doubles the respective trend in the previous 1982–2011 period ($0.029\,^{\circ}\mathrm{C\,yr}^{-1}$).

The AW depth time series (Fig. 5) show a heterogeneous trend in the Mediterranean Sea, with significant negative values (the depth decreases) in the Algerian and Ionian sub-basins and positive values in the Tyrrhenian and Levantine regions (Table 1), which reflects into a tendency of the AW to become shallower, increasing the stratification at basin scale

Table 1. Trends by year for the AW and LIW salinity, temperature, and depth time series in eight Mediterranean sub-basins. The trends that are significant at a 5 % level are shown in bold. The rightmost column shows the mean and standard deviation trend values computed over the eight sub-basins (here identified with MED). Trends are defined as mean ± standard deviation.

	Algerian	Catalan	Ligurian	Tyrrhenian	Adriatic	Ionian	Cretan	Levantine	MED
Salinity [yr^{-1}]									
AW	**−0.014 ± 0.151**	**−0.004 ± 0.088**	-0.001 ± 0.089	**0.006 ± 0.157**	**0.044 ± 0.188**	**0.009 ± 0.181**	**0.013 ± 0.166**	**0.003 ± 0.100**	**0.007 ± 0.140**
LIW	**0.002 ± 0.022**	**0.002 ± 0.017**	**0.005 ± 0.034**	**0.006 ± 0.035**	**0.021 ± 0.074**	**0.004 ± 0.031**	**0.005 ± 0.048**	**0.004 ± 0.039**	**0.006 ± 0.038**
Temperature [$^{\circ}\mathrm{C\,yr}^{-1}$]									
AW	**0.054 ± 0.614**	0.019 ± 0.846	0.004 ± 0.914	**0.042 ± 0.528**	**0.117 ± 0.951**	**0.023 ± 0.395**	**−0.026 ± 0.786**	**0.026 ± 0.683**	**0.026 ± 0.715**
LIW	**0.008 ± 0.125**	**0.010 ± 0.088**	**0.022 ± 0.138**	**0.030 ± 0.167**	**0.093 ± 0.384**	**0.030 ± 0.226**	-0.003 ± 0.226	**0.012 ± 0.391**	**0.022 ± 0.232**
Depth [$\mathrm{m\,yr}^{-1}$]									
AW	**−0.092 ± 2.271**	-0.019 ± 4.646	-0.012 ± 5.720	**0.394 ± 4.002**	0.757 ± 25.800	**−0.324 ± 7.352**	0.116 ± 17.480	**1.087 ± 17.024**	**0.238 ± 10.537**
LIW	-0.352 ± 14.639	**1.895 ± 52.582**	-0.155 ± 40.249	**−7.034 ± 46.395**	2.609 ± 115.404	**−4.973 ± 42.536**	**−1.630 ± 26.943**	**0.849 ± 32.912**	**1.099 ± 46.458**

($0.238 \pm 10.537\,\mathrm{m\,yr^{-1}}$). Wider temporal changes are found in the Levantine region, where the trend is 1 to 2 orders of magnitude higher than the other regions.

3.3.2 LIW

The LIW temporal variability will now be analysed. Figure 6 shows the salinity changes from 2001 to 2019 in the eight sub-basins considered. A positive trend is found in the whole Mediterranean Sea at a 5 % level of significance, highlighting an additional salinification at intermediate depths of this enclosed basin over 2 decades ($\sim 0.006 \pm 0.038\,\mathrm{yr^{-1}}$; Table 1). A similar positive trend between 150–600 m is found by Skliris et al. (2018) in the MEDATLAS data from 1950 to 2002 ($\sim 0.007 \pm 0.004\,\mathrm{yr^{-1}}$) with lower standard deviations. The higher standard deviations found in this study compared to those founds by Skliris et al. (2018) could be related to the wider range of depths considered and the different epochs considered. The LIW properties vary less than those of AW in most of the basin, except for the Ligurian and Levantine regions, where deep water and LIW water formations occur, respectively. The strongest salinity increase is found in the Adriatic Sea ($0.021 \pm 0.074\,\mathrm{yr^{-1}}$), exceeding the trends in other regions by an order of magnitude. The Adriatic salinity trend from 2008 to 2018 is about 5 times larger than the Adriatic salinity trend observed in the period 1952–2010 and quantified by Vilibić et al. (2013). The possible source of such a large trend may be due to the biassing of the signal by the BiOS oscillations since the series starts in 2008 when the anticyclonic BiOS was present. Here, the periodicity of the BiOS has a magnitude that is comparable to the time series length in the Adriatic, which might be also relevant for other sub-regions. Therefore, the longest time series are needed to better estimate the trend over this sub-basin.

The positive LIW salinity trends over the Mediterranean Sea are also found by Zu et al. (2014), which confirms the salinification of the basin at intermediate depths, as also observed at surface in most of the analysed regions. This suggests that the enhancement of the net evaporation over the Mediterranean in the last decades that was observed by Skiliris et al. (2018), may lead the formation of saltier LIW in the EMED and, as a consequence, a mean positive salinity trend over the whole basin. In contrast, in the WMED positive trends (0.008 ± 0.002; $0.009 \pm 0.0007\,\mathrm{yr^{-1}}$; from gliders missions) are found from 2011 to 2017 by Juza et al. (2019), in agreement with the positive trends found in the last few years in the western sub-basins shown in Fig. 6.

Positive temperature trends (5 % level of significance) are found in the whole Mediterranean Sea, except in the Levantine sub-basin, where the negative trend could be related to oscillations with decadal timescales that take place over this region. This is confirmed by the continuous wavelet transforms applied to the time series (not shown). Peaks of salinity and temperature are observed in ~ 2009 in the Levantine basin and then reach the Cretan Sea in ~ 2010. The same

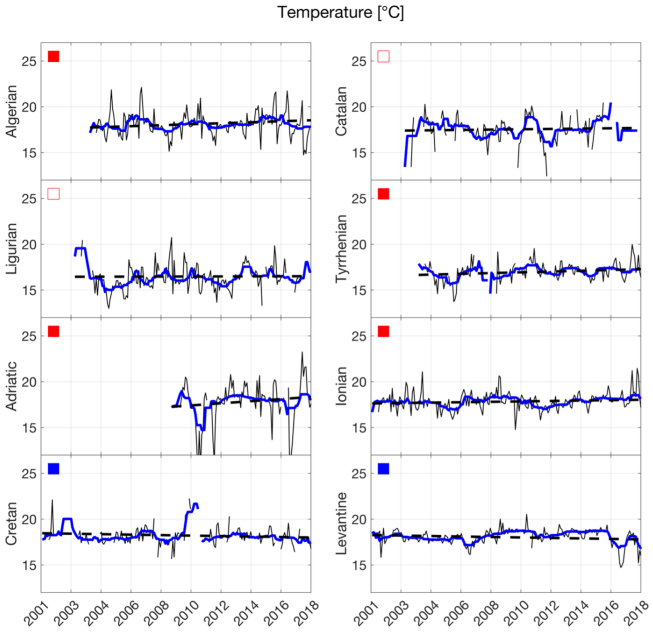

Figure 4. The same as Fig. 3 but for the AW temperature.

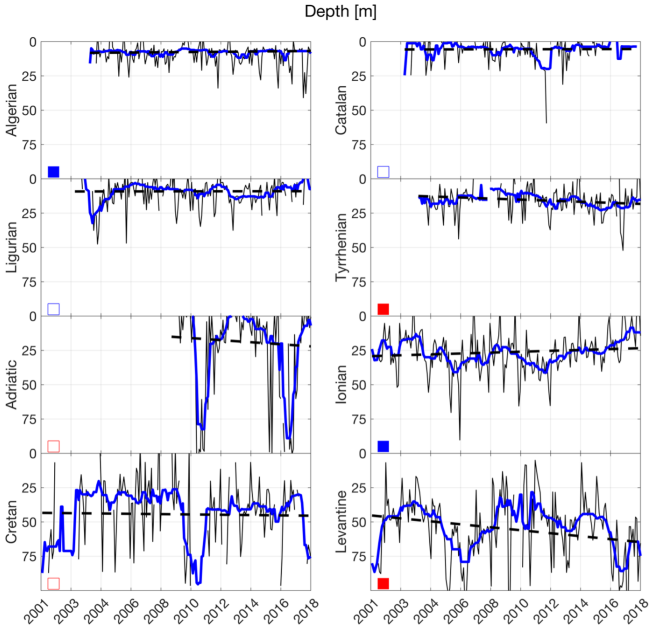

Figure 5. The same as Fig. 3 but for the AW depth. Positive and negative trends (red and blue squares, respectively) in this case correspond to an increase or decrease in depth (i.e. deeper or shallower), respectively.

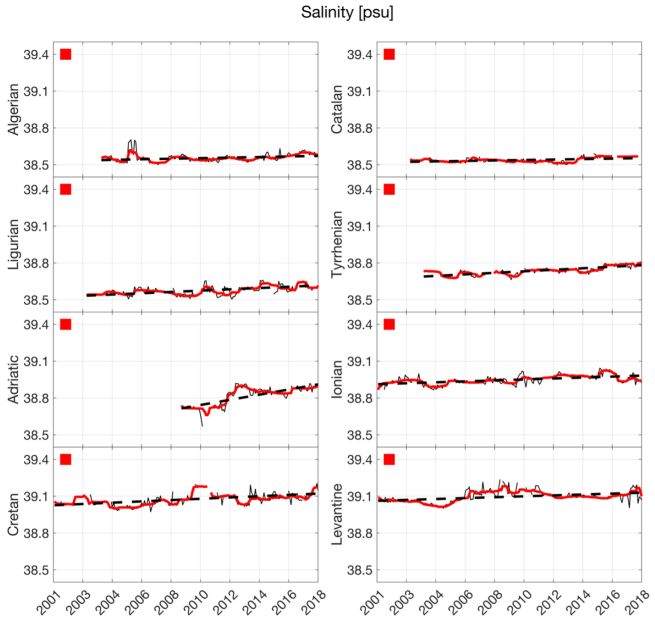

Figure 6. The same as Fig. 3 but for the LIW salinity.

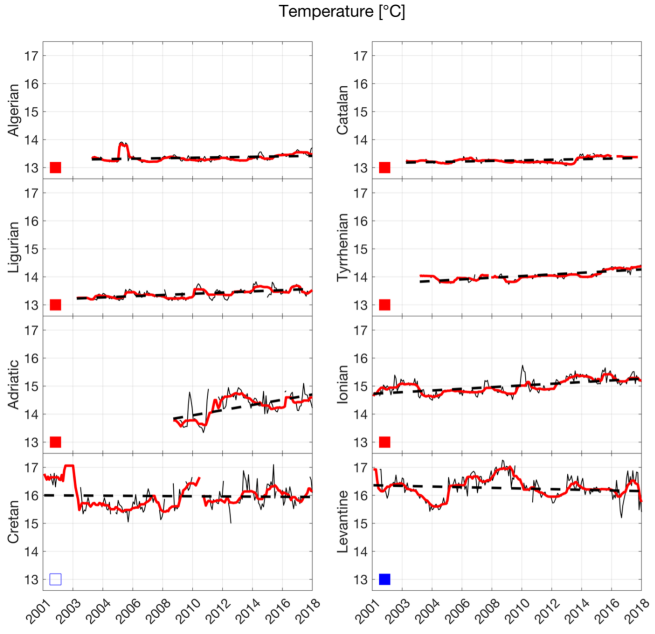

Figure 7. The same as Fig. 3 but for the LIW temperature.

variability is discussed in Ozer et al. (2017) and explained in connection with the Ionian Bimodal Oscillating System (BiOS). These maxima are in fact attributed to periods of anticyclonic circulation in the northern Ionian Sea (2006–2009) and limited AW advection in the southeastern Levantine basin, referring to the study by Artale et al. (2006). The LIW temperature mean trend and standard deviation averaged over the eight sub-basins is $\sim 0.002 \pm 0.232\,^{\circ}\mathrm{C\,yr^{-1}}$ (Table 1), which can be interpreted as a weaker response of the intermediate layers to the warming trend observed at surface.

The sub-basins with the steepest increase are located in the central longitudinal band of the Mediterranean Sea and are therefore far from the LIW main sources. The range of temperature and salinity and the respective variability in the Tyrrhenian and Ionian sub-basins are in good agreement with Poulain et al. (2009), where T and S time series from 2001 to 2009 are computed from Argo floats data near 600 m. The ranges and trends for T and S found in the Ligurian Sea are also confirmed by Margirier et al. (2020), where vertical profiles collected by gliders, Argo floats, CTD sensors, and XBTs in the northwestern Mediterranean Sea over the 2007–2017 period are analysed.

The LIW depth time series are shown in Fig. 8: significant negative trends (the depth decreases) are found in the Tyrrhenian, Ionian, and Cretan seas, while in the Catalan and Levantine sub-basins the LIW sinks (p value ≤ 0.05). Non-significant trends are found in the other regions. Abrupt shifts are found in the Adriatic sub-basin from ~ 200 to ~ 500–600 m at different time steps (trend $\sim 2.609 \pm 115.404\,\mathrm{m\,yr^{-1}}$), highlighting a bimodal behaviour of the LIW depth and an intense dense water production activity as also shown by Kokkini et al. (2019) and Mihanović et al. (2021). Previous studies attribute dramatic shifts in the Adriatic hydrological properties to the BiOS and the Eastern Mediterranean Transient (e.g. Vilibić et al., 2012). This hypothesis can also be supported by correlations between the BiOS (definition by Vilibić et al., 2020) and the AW and LIW yearly averaged salinity time series in the Adriatic Sea, which have maximum values that are about -0.49 and -0.43 at a lag of 0 -4 years (at negative year lag, the BiOS leads; p value ≤ 0.05), respectively. Further investigations are left to future studies.

The results related to the EMED match those shown in Kassis and Korres (2020), where the time series of salinity and temperature averaged between different depth layers (below 100 m) in similar sub-basins are shown (see Fig. 8 in Kassis and Korres, 2020). The LIW depth mean trend and standard deviation averaged over the eight sub-basins is $1.099 \pm 46.458\,\mathrm{m\,yr^{-1}}$ (Table 1).

4 Conclusions

We presented an analysis of the main properties and variability of the AW and LIW in the Mediterranean Sea, exploiting the Argo float data that provide an optimal observational dataset to study their thermohaline properties. Indeed, this dataset covers the water column down to ~ 2000 m and provides data for almost 2 decades.

Taking advantage of different diagnostics discussed in Sect. 2, AW and LIW have been detected in the Mediterranean Sea through a sub-basin approach, which allowed

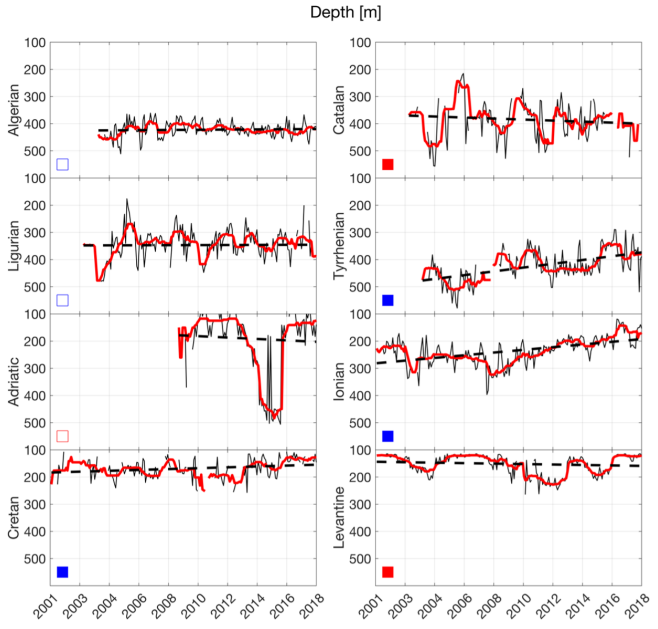

Figure 8. The same as Fig. 3 but for the LIW depth. Positive and negative trends (red and blue squares, respectively) in this case correspond to an increase and decrease of the depth (i.e. deeper or shallower), respectively.

to define the main hydrological features over this enclosed basin in different regions.

In addition to previous studies, this work provides a more detailed view of the AW and LIW characteristics in the last 2 decades over most of the Mediterranean Sea, except for the Alboran sub-basin, the Sicily Channel, and the Aegean sub-basin where Argo data are too scarce.

To achieve this goal, the first step of this study was the detection of the AW and LIW cores in each available profile. In agreement with previous studies (e.g. Lascaratos et al., 1993; Bergamasco and Malanotte-Rizzoli, 2010; Millot, 2013; Hayes et al., 2019; Vargas-Yáñez et al., 2020), we confirmed the mean zonal gradients of the AW and LIW properties over the Mediterranean Sea: AW becomes saltier, warmer, and deeper moving eastward, while LIW becomes fresher, colder, and deeper moving westward. These results not only match the present literature but also provide a more detailed view of these water masses over eight sub-basins.

The time series derived from the AW and LIW parameters have also highlighted some interesting features that are in good agreement with the previous literature. The most relevant results are summarized below.

- Positive salinity and temperature trends characterize AW and LIW in the last 2 decades over most of the Mediterranean Sea (average values over the whole region of 0.007 and 0.006 yr^{-1} and 0.026 and 0.022 $^{\circ}\mathrm{C\,yr}^{-1}$ respectively). The warming and salinification of the Mediterranean Sea is in good agreement with previous results (e.g. Skliris et al., 2018; Margirier et al., 2020; Kassis and Korres, 2020).

- Negative AW salinity trends in the Algerian and Catalan sub-basins suggest a freshening of the AW inflow, in agreement with the observed rapid freshening of the North Atlantic Ocean (Dickson et al., 2002).

- Positive AW salinity trends are found east of the Ligurian sub-basin, highlighting a clear salinification of this water mass in the last 2 decades that is probably due to the combined effect of the strong increase in net evaporation and the damming of the Nile (e.g. Nof, 1979; Skiliris et al., 2018; Sect. 3.3.1).

- Positive trends in the LIW salinity time series are found in the whole Mediterranean Sea at a 5 % level of significance, highlighting that salinification also exists at intermediate depths (Sect. 3.3.2).

- Positive LIW temperature trends (p value ≤ 0.05) are found everywhere except in the Levantine sub-basin, where the negative trend might be related to oscillations with decadal timescales that play a role in this region. These results highlight a clear warming at intermediate depths in most of the Mediterranean Sea.

- The AW and LIW depth trends are highly space dependent, showing different behaviours in the eight sub-basins.

- Abrupt shifts in the LIW depth are found in the Adriatic sub-basin from ~ 200 to ~ 500–600 m at different time steps (trend $2.609 \pm 115.404\,\mathrm{m\,yr}^{-1}$), highlighting a bimodal behaviour of the LIW depth and an intense dense water production activity, as also shown by Kokkini et al. (2019) and Mihanović et al. (2021).

- The time series length could affect the measurement of the trends in the sub-basins that are affected by periodicity forcings with the same order of magnitude. In this respect, the trends observed in the Adriatic Sea are clearly impacted by the BiOS since the time series starts in 2008 when the anticyclonic BiOS was present. This might be also relevant for other sub-regions.

These results therefore provide interesting new insights about the AW and LIW inter-basin and inter-annual variability that can be further analysed to investigate which mechanisms led to the observed temporal trends in each sub-basin.

Code availability. The analyses are performed with the MATLAB programming and numeric computing platform, developed by MathWorks (https://ch.mathworks.com/products/matlab.html, MathWorks, 2007). The codes have been implemented directly by the first author, and thus they are not available to other users.

Data availability. Data used in this paper are freely available from the International Argo Program and the national programs that contribute to it (https://argo.ucsd.edu, https://www.ocean-ops.org; https://archimer.ifremer.fr/doc/00652/76377/, Wong et al., 2020).

Author contributions. Conceptualization of the study was done by GF and PMP. GF prepared the original manuscript. GF, EM, GN, and PMP reviewed and edited the manuscript. GF, EM, GN, and PMP created the methodology. GF created the codes. GF performed the validation. GF performed the formal analysis. GF, EM, GN, and PMP conducted the investigation. GF and GN curated the data. EM, GN, and PMP provided supervision. EM was responsible for project administration. EM was responsible for funding acquisition. All authors have read and agreed to the published version of the paper.

Competing interests. The contact author has declared that neither they nor their co-authors have any competing interests.

Disclaimer. Publisher's note: Copernicus Publications remains neutral with regard to jurisdictional claims in published maps and institutional affiliations.

Special issue statement. This article is part of the special issue "Advances in interdisciplinary studies at multiple scales in the Mediterranean Sea". It is a result of the 8th MONGOOS Meeting & Workshop, Trieste, Italy, 3–5 December 2019.

Acknowledgements. This research was funded by the Italian Ministry of University and Research as part of the ARGO-ITALY program.

Financial support. This research has been supported by the Ministero dell'Istruzione, dell'Università e della Ricerca (MOCCA project, grant no. EASME/EMFF/2015/1.2.1.1/SI2.70962).

Review statement. This paper was edited by Alejandro Orfila and reviewed by three anonymous referees.

References

Argo: Argo float data and metadata from Global Data Assembly Centre (Argo GDAC), SEANOE [data set], https://doi.org/10.17882/42182, 2020.

Artale, V., Calmante, S., Malanotte-Rizzoli, P., Pisacane, G., Rupolo, V., and Tsimplis, M.: The Atlantic and Mediterranean Sea as connected systems, in: Mediterranean Climate Variability Dev. Earth Environ. Sci., edited by: Lionello, P., Malanotte-Rizzoli, P., and Boscoli, R., Vol. 4, Elsevier, Amsterdam, 283–323, 2006.

Aulicino, G., Cotroneo, Y., Ruiz, S., Sánchez Román, A., Pascual, A., Fusco, G., Tintoré, J., and Budillon, G.: Monitoring the Algerian Basin through glider observations, satellite altimetry and numerical simulations along a SARAL/AltiKa track, J. Marine Syst., 179, 55–71, https://doi.org/10.1016/j.jmarsys.2017.11.006, 2018.

Aulicino, G., Cotroneo, Y., Olmedo, E., Cesarano, C., Fusco, G., and Budillon, G.: In Situ and Satellite Sea Surface Salinity in the Algerian Basin Observed through ABACUS Glider Measurements and BEC SMOS Regional Products, Remote Sens.-Basel, 11, 1361, https://doi.org/10.3390/rs11111361, 2019.

Azzaro, M., La Ferla, R., Maimone, G., Monticelli, L. S., Zaccone, R., and Civitarese, G.: Prokaryotic dynamics and heterotrophic metabolism in a deep convection site of Eastern Mediterranean Sea (the Southern Adriatic Pit), Cont. Shelf Res., 44, 106–118, https://doi.org/10.1016/j.csr.2011.07.011, 2012.

Bensi, M., Cardin, V., Rubino, A., Notarstefano, G., and Poulain, P. M.: Effects of winter convection on the deep layer of the Southern Adriatic Sea in 2012, J. Geophys. Res.-Oceans, 118, 6064–6075, https://doi.org/10.1002/2013JC009432, 2013.

Bergamasco, A. and Malanotte-Rizzoli, P.: The circulation of the Mediterranean Sea: A historical review of experimental investigations, Advances in Oceanography and Limnology, 1, 11–28, https://doi.org/10.1080/19475721.2010.491656, 2010.

Borghini, M., Bryden, H., Schroeder, K., Sparnocchia, S., and Vetrano, A.: The Mediterranean is becoming saltier, Ocean Sci., 10, 693–700, https://doi.org/10.5194/os-10-693-2014, 2014.

Bosse, A., Testor, P., Mortier, L., Prieur, L., Taillandier, V., d'Ortenzio, F., and Coppola, L.: Spreading of Levantine Intermediate Waters by submesoscale coherent vortices in the northwestern Mediterranean Sea as observed with gliders, J. Geophys. Res.-Oceans, 120, 1599–1622, https://doi.org/10.1002/2014JC010263, 2015.

Bethoux, J. P., Gentili, B., Raunet, J., and Taillez, D.: Warming trend in the Western Mediterranean deep water, Nature, 347, 660–662, https://doi.org/10.1038/347660a0, 1990.

Bethoux, J. P., Gentili, B., Morin, P., Nicolas, E., Pierre, C., and Ruiz-Pino, D.: The Mediterranean Sea: A miniature ocean for climatic and environmental studies and a key for the climatic functioning of the North Atlantic, Prog. Oceanogr., 44, 131–146, https://doi.org/10.1016/S0079-6611(99)00023-3, 1999.

Cabanes, C., Thierry, V., and Lagadec, C.: Improvement of bias detection in Argo float conductivity sensors and its application in the North Atlantic, Deep-Sea Res. Pt. I, 114, 128–136, https://doi.org/10.1016/j.dsr.2016.05.007, 2016.

Cotroneo, Y., Aulicino, G., Ruiz, S., Pascual, A., Budillon, G., Fusco, G., and Tintoré, J.: Glider and satellite high resolution monitoring of a mesoscale eddy in the algerian basin: Effects on the mixed layer depth and biochemistry, J. Marine Syst., 162, 73–88, https://doi.org/10.1016/j.jmarsys.2015.12.004, 2016.

Cotroneo, Y., Aulicino, G., Ruiz, S., Sánchez Román, A., Torner Tomàs, M., Pascual, A., Fusco, G., Heslop, E., Tintoré, J., and Budillon, G.: Glider data collected during the Algerian Basin Circulation Unmanned Survey, Earth Syst. Sci. Data, 11, 147–161, https://doi.org/10.5194/essd-11-147-2019, 2019.

Demirov, E. K. and Pinardi, N.: On the relationship between the water mass pathways and eddy variability in the Western Mediterranean Sea, J. Geophys. Res., 112, C02024, https://doi.org/10.1029/2005JC003174, 2007.

Dickson, B., Yashayaev, I., Meincke, J., Turrell, B., Dye, S., and Holfort, J.: Rapid freshening of the deep North Atlantic Ocean over the past four decades, Nature, 416, 832–837, https://doi.org/10.1038/416832a, 2002.

Dukhovskoy, D. S., Yashayaev, I., Proshutinsky, A., Bamber, J. L., Bashmachnikov, I. L., Chassignet, E. P., Lee, C. M., and Tedstone, A. J.: Role of Greenland freshwater anomaly in the recent freshening of the subpolar North Atlantic, J. Geophys. Res.-Oceans, 124, 3333–3360, https://doi.org/10.1029/2018JC014686, 2019.

Escudier, R., Mourre, B., Juza, M., and Tintoré, J.: Subsurface circulation and mesoscale variability in the Algerian subbasin from altimeter-derived eddy trajectories, J. Geophys. Res.-Oceans, 121, 6310–6322, https://doi.org/10.1002/2016JC011760, 2016.

Font, J., Millot, C., Pérez, J. D. J. S., Julià, A., and Chic, O.: The drift of Modified Atlantic Water from the Alboran Sea to the eastern Mediterranean, Sci. Mar., 62, 211–216, https://doi.org/10.3989/scimar.1998.62n3211, 1998.

Giorgi, F.: Climate change hot-spots, Geophys. Res. Lett., 33, L08707, https://doi.org/10.1029/2006GL025734, 2006.

Hayes, D. R., Schroeder, K., Poulain, P. M., Testor, P., Mortier, L., Bosse, A., and Du Madron, X.: Review of the Circulation and Characteristics of Intermediate Water Masses of the Mediterranean: Implications for Cold-Water Coral Habitats, in: Mediterranean Cold-Water Corals: Past, Present and Future, edited by: Orejas, C. and Jiménez, C., Coral Reefs of the World, Vol. 9, Springer, Cham, https://doi.org/10.1007/978-3-319-91608-8_18, 2019.

Hernández-Molina, F., Stow, D., Zarikian, C., Acton, G., Bahr, A., Balestra, B., Ducassou, E., Flood, R., Flores, J. A., Furota, S., Grunert, P., Hodell, D., Jiménez-Espejo, F., Kim, J. K., Krissek, L., Kuroda, J., Li, B., Llave, E., Lofi, J., and Xuan, C.: Onset of Mediterranean outflow into the North Atlantic, Science, 344, 1244–1250, https://doi.org/10.1126/science.1251306, 2014.

Juza, M., Escudier, R., Vargas-Yáñez, M., Mourre, B., Heslop, E., Allen, J., and Tintoré, J.: Characterization of changes in Western Intermediate water properties enabled by an innovative geometry-based detection approach, J. Marine Syst., 191, 1–12, https://doi.org/10.1016/j.jmarsys.2018.11.003, 2019.

Kassis, D. and Korres, G.: Hydrography of the Eastern Mediterranean basin derived from argo floats profile data, Deep-Sea Res. Pt. II, 171, 104712, https://doi.org/10.1016/j.dsr2.2019.104712, 2020.

Kokkini, Z., Mauri, M., Gerin, R., Poulain, P. M., Simoncelli, S., and Notarstefano, G.: On the salinity structure in the South Adriatic as derived from float and glider observations in 2013–2016, Deep-Sea Res. Pt. II, 171, 104625, https://doi.org/10.1016/j.dsr2.2019.07.013, 2019.

Kubin, E., Poulain, P.-M., Mauri, E., Menna, M., and Notarstefano, G.: Levantine Intermediate and Levantine Deep Water Formation: An Argo Float Study from 2001 to 2017, Water, 11, 1781, https://doi.org/10.3390/w11091781, 2019.

Lamer, P. A., Mauri, E., Notarstefano, G., and Poulain, P. M.: The Levantine Intermediate Water in the eastern Mediterranean Sea, available at: http://maos.inogs.it/pub/REPORT_LAMER_final_last.pdf (last access: December 2021), 2019.

Lascaratos, A., Williams, R. G., and Tragou, E.: A mixed-layer study of the formation of Levantine intermediate water, J. Geophys. Res., 98, 14739–14749, https://doi.org/10.1029/93JC00912, 1993.

Lipizer, M., Partescano, E., Rabitti, A., Giorgetti, A., and Crise, A.: Qualified temperature, salinity and dissolved oxygen climatologies in a changing Adriatic Sea, Ocean Sci., 10, 771–797, https://doi.org/10.5194/os-10-771-2014, 2014.

Margirier, F., Testor, P., Heslop, E., Mallil, K., Bosse, A., Houpert, L., Mortier, L., Bouin, M.-N., Coppola, L., D'Ortenzio, F., de Madron, X. D., Mourre, B., Prieur, L., Raimbault, P., and Taillandier, V.: Abrupt warming and salinification of intermediate waters interplays with decline of deep convection in the Northwestern Mediterranean Sea, Sci. Rep.-UK, 10, 20923, https://doi.org/10.1038/s41598-020-77859-5, 2020.

Mauri, E., Sitz, L., Gerin, R., Poulain, P. M., Hayes, D., and Gildor, H.: On the Variability of the Circulation and Water Mass Properties in the Eastern Levantine Sea between September 2016–August 2017, Water, 11, 1741, https://doi.org/10.3390/w11091741, 2019.

Mauri, E., Menna, M., Notarstefano, G., Gerin, R., Martellucci, R., and Poulain, P.-M.: Recent changes of the salinity distribution in the South Adriatic, EGU General Assembly 2020, Online, 4–8 May 2020, EGU2020-9874, https://doi.org/10.5194/egusphere-egu2020-9874, 2020.

MEDAR Group: MEDATLAS/2002 database, Mediterranean and Black Sea database of temperature salinity and bio-chemical parameters, Climatological Atlas, Institut Français de Recherche pour L'Exploitation de la Mer, (IFREMER) Edition & Instituto Nazionale di Oceanografia e di Geofisica Sperimentale (OGS), 2002.

Mihanović, H., Vilibić, I., Šepić, J., Matić, F., Ljubešić, Z., Mauri, E., Gerin, R., Notarstefano, G., and Poulain, P.-M.: Observation, preconditioning and recurrence of exceptionally high salinities in the Adriatic Sea, Front. Mar. Sci., 8, 672210, https://doi.org/10.3389/fmars.2021.672210, 2021.

Millot, C.: Interannual salinification of the Mediterranean inflow, Geophys. Res. Lett., 34, L21609, https://doi.org/10.1029/2007GL031179, 2007.

Millot, C.: Levantine Intermediate Water characteristics: An astounding general misunderstanding, Sci. Mar., 78, https://doi.org/10.3989/scimar.04045.30H, 2013.

Millot, C.: Levantine intermediate water characteristics: an astounding general misunderstanding! (addendum), Sci. Mar., 78, 165–171, https://doi.org/10.3989/scimar.04045.30H, 2014.

Millot, C. and Taupier-Letage, I.: Circulation in the Mediterranean Sea, in: The Mediterranean Sea. Handbook of Environmental Chemistry, edited by: Saliot, A., Vol. 5K, Springer, Berlin, Heidelberg, https://doi.org/10.1007/b107143, 2005.

Millot, C., Candela, J., Fuda, J. L., and Tber, Y.: Large warming and salinification of the Mediterranean outflow due to changes in its composition, Deep-Sea Res., 53, 656–665, https://doi.org/10.1016/j.dsr.2005.12.017, 2006.

Nof, D.: On man-induced variations in the circulation of the Mediterranean Sea, Tellus, 31, 558–564, 1979.

Notarstefano, G. and Poulain, P. M.: Delayed mode quality control of Argo floats salinity data in the Tyrrhenian Sea, Technical Report OGS 2008/125 OGA 43 SIRE, available at: http://nettuno.ogs.trieste.it/sire/DMQC/dmqc_1900593_54073_V1.pdf (last access: December 2021), 2008.

Notarstefano, G. and Poulain, P. M.: Thermohaline variability in the Mediterranean and Black Seas as observed by Argo floats in 2000–2009, OGS Tech. Rep. OGS 2009/121 OGA 26 SIRE, 72–171, https://doi.org/10.3989/scimar.04045.30H, 2009.

Notarstefano, G. and Poulain, P. M.: Delayed mode quality control of Argo salinity data in the Mediterranean Sea: A regional approach, Technical Report OGS 2013/103 Sez. OCE 40 MAOS, available at: http://nettuno.ogs.trieste.it/sire/DMQC/dmqc_1900604_63659_V1.pdf (last access: 17 January 2022), 2013.

Ozer, T., Gertman, I., Kress, N., Silverman, J., and Herut, B.: Interannual thermohaline (1979–2014) and nutrient (2002–2014) dynamics in the Levantine surface and intermediate water masses, SE Mediterranean Sea, Global Planet. Change, 151, 60–67, https://doi.org/10.1016/j.gloplacha.2016.04.001, 2017.

Painter, S. C. and Tsimplis, M. N.: Temperature and salinity trends in the upper waters of the Mediterranean Sea as determined from the MEDATLAS dataset, Cont. Shelf Res., 23, 1507–1522, https://doi.org/10.1016/j.csr.2003.08.008, 2003.

Pearson, K.: Contributions to the Mathematical Theory of Evolution. II. Skew Variation in Homogeneous Material, Philos. T. R. Soc. A, 186, 343–414, https://doi.org/10.1098/rsta.1895.0010, 1895.

Poulain, P.-M., Barbanti, R., Font, J., Cruzado, A., Millot, C., Gertman, I., Griffa, A., Molcard, A., Rupolo, V., Le Bras, S., and Petit de la Villeon, L.: MedArgo: a drifting profiler program in the Mediterranean Sea, Ocean Sci., 3, 379–395, https://doi.org/10.5194/os-3-379-2007, 2007.

Poulain, P. M., Solari, M., Notarstefano, G., and Rupolo, V.: Assessment of the Argo sampling in the Mediterranean and Black Seas (part II), available at: http://maos.inogs.it/pub/2009_report_task4.4_partII.pdf (last access: December 2021), 2009.

Rahmstorf, S.: Influence of Mediterranean Outflow on climate, EOS T. Am. Geophys. Un., 79, 281–282, https://doi.org/10.1029/98EO00208, 1998.

Rahmstorf, S.: Thermohaline Ocean Circulation, in: Encyclopedia of Quaternary Sciences, edited by: Elias, S. A., Elsevier, Amsterdam, available at: http://www.pik-potsdam.de/~stefan/Publications/Book_chapters/rahmstorf_eqs_2006.pdf (last access: December 2021), 2006.

Rohling, E. J. and Bryden, H. L.: Man induced salinity and temperature increase in the Western Mediterranean Deep Water, J. Geophys. Res., 97, 11191–11198, https://doi.org/10.1029/92JC00767, 1992.

Rubino, A., Gačić, M., Bensi, M., Vedrana, K., Vlado, M., Milena, M., Negretti, M. E., Sommeria, J., Zanchettin, D., Barreto, R. V., Ursella, L., Cardin, V., Civitarese, G., Orlić, M., Petelin, B., and Siena, G.: Experimental evidence of long-term oceanic circulation reversals without wind influence in the North Ionian Sea, Sci. Rep.-UK, 10, 1905, https://doi.org/10.1038/s41598-020-57862-6, 2020.

Schroeder, K.: Current Systems in the Mediterranean Sea, in: Encyclopedia of Ocean Sciences, edited by: Cochran, J. K., Bokuniewicz, H. J., and Yager, P. L., 3rd Edn., Academic Press, 219–227, https://doi.org/10.1016/B978-0-12-409548-9.11296-5, 2019.

Schroeder, K., Chiggiato, J., Josey, S., Borghini, M., Aracri, S., and Sparnocchia, S.: Rapid response to climate change in a marginal sea, Sci. Rep.-UK, 7, 4065, https://doi.org/10.1038/s41598-017-04455-5, 2017.

von Schuckmann, K., Le Traon, P., Smith, N., Pascual, A., Djavidnia, S., Gattuso, J.-P., Grégoire, M., Nolan, G., Aaboe, S., Aguiar, E., Álvarez Fanjul, E., Alvera-Azcárate, A., Aouf, L., Barciela, R., Behrens, A., Belmonte Rivas, M., Ben Ismail, S., Bentamy, A., Borgini, M., Brando, V. E., Bensoussan, N., Blauw, A., Bryère, P., Buongiorno Nardelli, B., Caballero, A., Çağlar Yumruktepe, V., Cebrian, E., Chiggiato, J., Clementi, E., Corgnati, L., de Alfonso, M., de Pascual Collar, Á., Deshayes, J., Di Lorenzo, E., Dominici, J.-M., Dupouy, C., Drévillon, M., Echevin, V., Eleveld, M., Enserink, L., García Sotillo, M., Garnesson, P., Garrabou, J., Garric, G., Gasparin, F., Gayer, G., Gohin, F., Grandi, A., Griffa, A., Gourrion, J., Hendricks, S., Heuzé, C., Holland, E., Iovino, D., Juza, M., Kurt Kersting, D., Kipson, S., Kizilkaya, Z., Korres, G., Kõuts, M., Lagemaa, P., Lavergne, T., Lavigne, H., Ledoux, J.-B., Legeais, J.-F., Lehodey, P., Linares, C., Liu, Y., Mader, J., Maljutenko, I., Mangin, A., Manso-Narvarte, I., Mantovani, C., Markager, S., Mason, E., Mignot, A., Menna, M., Monier, M., Mourre, B., Müller, M., Nielsen, J. W., Notarstefano, G., Ocaña, O., Pascual, A., Patti, B., Payne, M. R., Peirache, M., Pardo, S., Pérez Gómez, B., Pisano, A., Perruche, C., Peterson, K. A., Pujol, M.-I., Raudsepp, U., Ravdas, M., Raj, R. P., Renshaw, R., Reyes, E., Ricker, R., Rubio, A., Sammartino, M., Santoleri, R., Sathyendranath, S., Schroeder, K., She, J., Sparnocchia, S., Staneva, J., Stoffelen, A., Szekely, T., Tilstone, G. H., Tinker, J., Tintoré, J., Tranchant, B., Uiboupin, R., Van der Zande, D., von Schuckmann, K., Wood, R., Woge Nielsen, J., Zabala, M., Zacharioudaki, A., Zuberer, F., and Zuo, H.: Copernicus marine service ocean state report, J. Oper. Oceanogr., 12, S1–S123, https://doi.org/10.1080/1755876X.2019.1633075, 2019.

Shaltout, M. and Omstedt, A.: Recent sea surface temperature trends and future scenarios for the Mediterranean Sea, Oceanologia, 56, 411–443, https://doi.org/10.5697/oc.56-3.411, 2014.

MathWorks: MATLAB programming, PHI Learning Pvt. Ltd., available at: https://ch.mathworks.com/products/matlab.html (last access: December 2021), 2007.

Skliris, N.: Past, Present and Future Patterns of the Thermohaline Circulation and Characteristic Water Masses of the Mediterranean Sea, in: The Mediterranean Sea, edited by: Goffredo, S. and Dubinsky, Z., Springer, Dordrecht, https://doi.org/10.1007/978-94-007-6704-1_3, 2014.

Skliris, N., Zika, J. D., Herold, L., Josey, S. A., and Marsh, R.: Mediterranean sea water budget long-term trend inferred from salinity observations, Clim. Dynam., 51, 2857–2876, https://doi.org/10.1007/s00382-017-4053-7, 2018.

Tsimplis, M., Zervakis, V., Josey, S. A., Peneva, E., Struglia, M. V., Stanev, E., Lionello, P., Malanotte-Rizzoli, P., Artale, V., Theocharis, A., Tragou, E., and Oguz, T.: Changes in the oceanography of the Mediterranean Sea and their link to climate variability, in: Mediterranean climate variability, edited by: Lionello, P., Malanotte-Rizzoli, P., and Boscolo, R., Elsevier, Amsterdam, the Netherlands, 227–282, Developments in Earth and Environmental Sciences, Vol. 4, 438 pp., https://doi.org/10.1016/S1571-9197(06)80007-8, 2006.

Vargas-Yáñez, M., Moya, F., Tel, E., García-Martínez, M. C., Guerber, E., and Bourgeon, M.: Warming and salting of the Western Mediterranean during the second half of the XX century: incon-

sistencies, unknowns and the effect of data processing, Sci. Mar., 73, 7–28, https://doi.org/10.3989/scimar.2009.73n1007, 2009.

Vargas-Yáñez, M., Moya, F., García-Martínez, M. C., Tel, E., Zunino, P., Plaza, F., Salat, J., Pascual, J., López-Jurado, J. L., and Serra, M.: Climate change in the Western Mediterranean Sea 1900–2008, J. Marine Syst., 82, 171–176, https://doi.org/10.1016/j.jmarsys.2010.04.013, 2010.

Vargas-Yáñez, M., Juza, M., Balbín, R., Velez-Belchí, P., García-Martínez, M. C., Moya, F., and Hernández-Guerra, A.: Climatological Hydrographic Properties and Water Mass Transports in the Balearic Channels From Repeated Observations Over 1996–2019, Front. Mar. Sci., 7, 568602, https://doi.org/10.3389/fmars.2020.568602, 2020.

Vilibić, I., Matijević, S., Šepić, J., and Kušpilić, G.: Changes in the Adriatic oceanographic properties induced by the Eastern Mediterranean Transient, Biogeosciences, 9, 2085–2097, https://doi.org/10.5194/bg-9-2085-2012, 2012.

Vilibić, I., Šepić, J., and Proust, N.: Weakening of thermohaline circulation in the Adriatic Sea, Clim. Res., 55, 217–225, 2013.

Vilibić, I., Zemunik, P., Dunić, N., and Mihanović, H.: Local and remote drivers of the observed thermohaline variability on the northern Adriatic shelf (Mediterranean Sea), Cont. Shelf Res., 199, 104110, https://doi.org/10.1016/j.csr.2020.104110, 2020.

Wong, A. P. S., Wijffels, S. E., Riser, S. C., Pouliquen, S., Hosoda, S., Roemmich, D., Gilson, J., Johnson, G. C., Martini, K., Murphy, D. J., Scanderbeg, M., Bhaskar, T. V. S. U., Buck, J. J. H., Merceur, F., Carval, T., Maze, G., Cabanes, C., André, X., Poffa, N., Yashayaev, I., Barker, P. M., Guinehut, S., Belbéoch, M., Ignaszewski, M., O'Neil Baringer, M., Schmid, C., Lyman, J. M., McTaggart, K. E., Purkey, S. G., Zilberman, N., Alkire, M. B., Swift, D., Owens, W. B., Jayne, S. R., Hersh, C., Robbins, P., West-Mack, D., Bahr, F., Yoshida, S., Sutton, P. J. H., Cancouët, R., Coatanoan, C., Dobbler, D., Juan Andrea, G., Gourrion, J., Kolodziejczyk, N., Bernard, V., Bourlès, B., Claustre, H., D'Ortenzio, F., Le Reste, S., Le Traon, P.-Y., Rannou, J. P., Saout-Grit, C., Speich, S., Thierry, V., Verbrugge, N., Angel-Benavides, I. M., Klein, B., Notarstefano, G, Poulain, P.-M., Vélez-Belchí, P., Suga, T., Ando, K., Iwasaska, N, Kobayashi, T., Masuda, S., Oka, E., Sato, K., Nakamura, T., Sato, K., Takatsuki, Y., Yoshida, T., Cowley, R., Lovell, J. L., Oke, P. R., Van Wijk, E. M., Carse, F., Donnelly, M., Gould, W. J., Gowers, K., King, B. A., Loch, S. G., Mowat, M., Turton, J., Rama, R. E. P., Ravichandran, M., Freeland, H. J., Gaboury, I., Gilbert, D., Greenan, B. J. W., Ouellet, M., Ross, T., Tran, A., Dong, M., Liu, Z., Xu, J., Kang, K., Jo, H., Kim, S.-D., and Park, H.-M.: Argo Data 1999–2019: Two Million Temperature-Salinity Profiles and Subsurface Velocity Observations From a Global Array of Profiling Floats, Front. Mar. Sci., 7, 700, https://doi.org/10.3389/fmars.2020.00700, 2020 (data available at: https://archimer.ifremer.fr/doc/00652/76377/, last access: 17 January 2022).

Wong, A., Keeley, R., Carval, T., and Argo Data Management Team: Argo Quality Control Manual for CTD and Trajectory Data, Argo, report, https://doi.org/10.13155/33951, 2021.

Zu, Z., Poulain, P. M., and Notarstefano, G.: Changes in hydrological properties of the Mediterranean Sea over the last 40 years with focus on the Levantine Intermediate Water and the Atlantic Water, available at: http://maos.inogs.it/pub/Hydro_trend_LIW_SAW_core_report_v10.pdf (last access: December 2021), 2014.